

## SHORT COMMUNICATION

**Breakdown and crystallization processes in niobium oxide films in oxalic acid solution**

M. B. J. G. FREITAS, L. O. S. BULHÕES\*

*Laboratório Interdisciplinar de Eletroquímica e Cerâmica, Departamento de Química, Universidade Federal de São Carlos, Caixa Postal 676, 13565-905, São Carlos-S.P., Brazil*

Received 19 September 1995; revised 29 October 1996

**1. Introduction**

Niobium has high corrosion resistance and is a useful alloying element in special steels. This corrosion resistance is due to a readily formed, adherent, passive film which inhibits dissolution through the film [1]. Anodic films formed on valve metals during the growth process in high electrical fields may suffer electrical or mechanical breakdown [2–6], depending on the solution composition, current density and temperature of the solution. Electrical breakdown is a consequence of electron avalanche [2, 4, 5] and mechanical breakdown occurs due to an increase in the strength of the film promoted by the electrical field and by interfacial tension [2, 7].

In this paper we describe an investigation of the electrochemical response of niobium in oxalic acid media during anodic polarization using the galvanostatic technique. A correlation between the electrolyte and the electrochemical response of the niobium electrode is discussed. The films obtained under different polarization conditions were analysed by X-ray diffraction analysis and electron scanning microscopy, and the state and composition of the oxide were determined by X-ray photoelectron spectroscopy.

**2. Experimental details**

Niobium electrodes were prepared from a niobium rod (99.9% m/m, CBMM, Brazil) with a geometric area of 0.28 cm<sup>2</sup>, or from a rectangular niobium sheet (0.2 mm thick) with a geometric area of 1.0 cm<sup>2</sup>. Before each electrochemical experiment the electrode surface was degreased in acetone, polished with 600 grit sandpaper, and then rinsed with distilled water.

The solutions were prepared with Milli-Q water and oxalic acid (p.a., Merck), and were deoxygenated with pure nitrogen before use. The galvanostatic experiments were performed with a regulated power supply, and the potential drop between the anode and auxiliary electrode was recorded by means of an ECB model RB 101  $x-t$  recorder.

X-ray photoelectron spectroscopy (XPS) measurements were carried out using a McPhearsen Company ESCA-36 with AlK<sub>α</sub> radiation. The pressure in the spectrometer chamber was 10<sup>-7</sup> torr and the binding energies were calibrated using C 1s

(285.0 eV) as the reference. X-ray diffractograms were taken on a Rigaku RU-200 B diffractometer, using CuK<sub>α</sub> radiation and a nickel filter. Before the XPS measurements the electrodes were maintained under dynamic vacuum for 10 h. All electrochemical experiments were performed at 25 °C.

**3. Results and discussion**

Figure 1 shows the potential as a function of time for the niobium electrode in aqueous solution with different oxalic acid contents. The increase of the potential with time indicates that the film increases in thickness. The higher electrode potential observed for more diluted solutions indicates that this film is thicker and that the current density inside the film is higher. In more concentrated solutions the dissolution rate probably increases, giving a higher dissolution current density and a thinner film. In this region, due to an increase in film thickness, interference colours are observed [1]. The anodization rate ( $dE/dt$ ) increases with the current density, as shown in Fig. 2, and no discernible effect on this parameter is observed with increasing electrolyte concentration. Figure 2 indicates that the growth rate has a polynomial dependence on the current density. During the film growth in the linear region of the potential–time curve, no oxygen discharge at the electrode surface is observed, as has been previously described for other valve metals [8, 9].

The decrease in the anodization rate in the growth curve is promoted by the decrease in the current density of the film. The current density of the film ( $i_f$ ) is given by the relation:

$$i_f = i - (i_d + i_e)$$

where  $i$  is the imposed current density,  $i_d$  the dissolution current density, and  $i_e$  the current density associated with electrolyte oxidation.

In solutions with different electrolyte concentrations, the shapes of the potential–time curves are practically the same. After the decay in the anodization rate (close to 300 V), the potential increases to a maximum and remains almost constant. The system reaches a steady state condition where the current density of the film ( $i_f$ ) becomes equal to that associated with film dissolution ( $i_d$ ) and electronic current density ( $i_e$ ) which stops the film growth. In this region, sparks at the electrode surface are observed

\* Author to whom correspondence should be addressed.

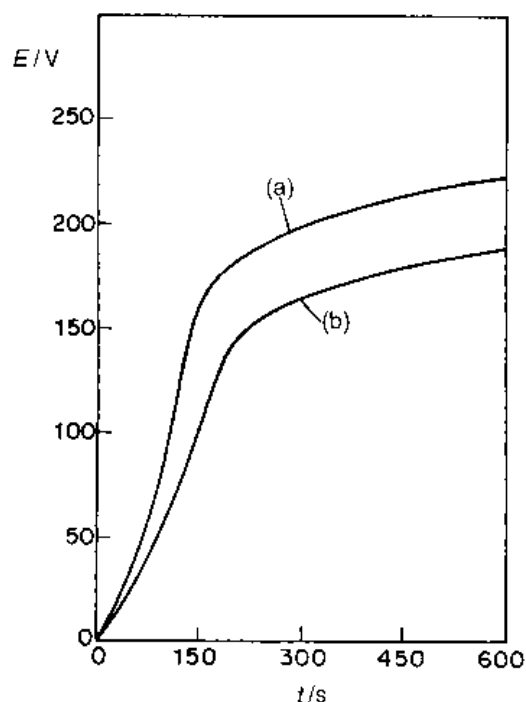


Fig. 1. Chronopotentiometric curves for the Nb electrode polarized at  $i = 8.0 \text{ mA cm}^{-2}$  in aqueous solution with oxalic acid: (a) 0.001 M and (b) 0.01 M.

due to an increase in the electronic current density, leading to the electron avalanche process which may promote breakdown of the film [4]. Figure 3 shows the chronopotentiometric curve for the niobium electrode during the breakdown process. To determine the origin of the breakdown phenomenon we determined the breakdown voltage as a function of electrolyte content. The breakdown potentials, measured at the plateau of the potential against time curves, are independent of the oxalic acid content.

The potential decay observed for polarization times higher than 1500 s is associated with the partial rupture of the film, followed by the reconstruction of

the oxide film. In this region, the ageing of the film increases the internal stresses to a level which cannot be tolerated by the mechanical strength of the film, thus promoting film rupture. Using electron microscopy it was possible to observe the presence of small fissures in the anodic film, as shown in Fig. 4. The oxide surface exhibits many small fissures and areas with large prominent fractures. To the naked eye the sample appears to be a dull homogeneous grey film.

No  $\text{C}_2\text{O}_4^{2-}$  was found inside the film by means of X-ray photoelectron spectroscopy measurements, indicating an excellent correlation with the galvanostatic experiments. The O/Nb ratio was 2.5, and the binding energies for Nb 3d and O 1s were 210.1 and 207.6 eV and 532.6 and 530.5 eV, respectively, in agreement with the expected values for niobium oxide [10]. The absence of  $\text{C}_2\text{O}_4^{2-}$  inside the film, also confirmed by the O/Nb ratio and by the absence of carbon in the samples in these investigated conditions, indicates that the breakdown phenomenon is limited to the bulk properties of the film, and occurs due to the increase in the mechanical strength of the film.

The structures of the anodic films were determined by X-ray diffraction analysis using niobium foils polished with 600 grit sandpaper, and with the film prepared by the galvanostatic technique in aqueous solution with 0.1 M  $\text{H}_2\text{C}_2\text{O}_4$  as the electrolyte. The crystallization was observed only for films prepared after prolonged anodization time ( $> 1000$  s). At polarization times less than 1000 s the diffractograms exhibit well-defined Nb peaks at  $38.4^\circ$  (100%),  $55.6^\circ$  (39%), and  $69.5^\circ$  (18%). Broad peaks related to the oxide phase are observed, indicating the amorphous nature of the film. Figure 5 shows the X-ray diffraction patterns for the film obtained in aqueous solution with 0.1 M  $\text{H}_2\text{C}_2\text{O}_4$  after 2000 s of anodic polarization. The experimental data were compared with the ASTM Table [11], and we identified Nb ( $38.4^\circ$ ), NbO ( $44.5^\circ$ ) and  $\text{Nb}_2\text{O}_5$  ( $28.4^\circ$ ) with the latter having an orthorhombic structure. The pres-

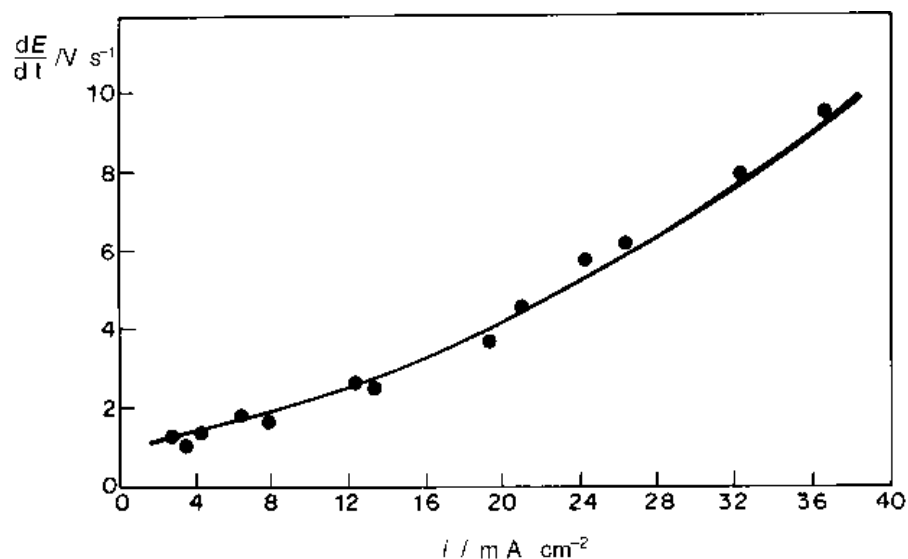


Fig. 2. The dependence of the growth rate ( $dE/dt$ ) as a function of the anodic current density for the Nb electrode in 0.1 M  $\text{H}_2\text{C}_2\text{O}_4$ .

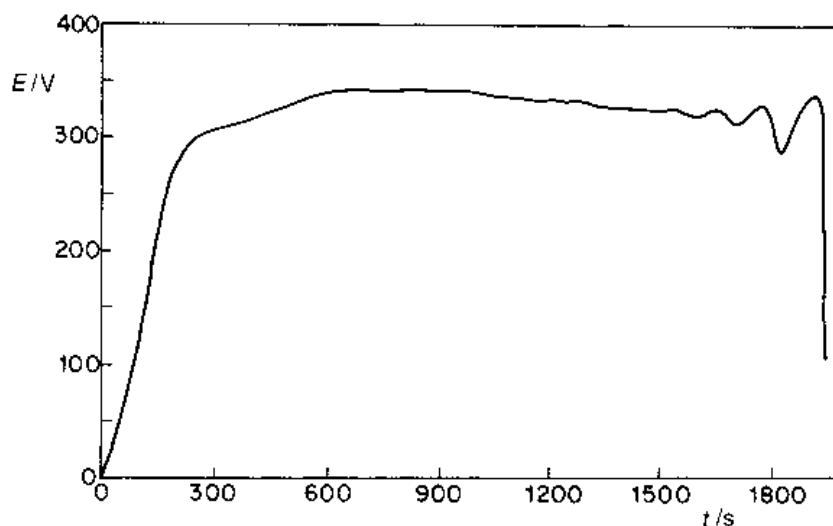


Fig. 3. Chronopotentiometric curves for Nb electrodes polarized with  $8 \text{ mA cm}^{-2}$  in  $0.1 \text{ M H}_2\text{C}_2\text{O}_4$ .



Fig. 4. SEM micrographs of niobium oxide film growth in  $0.1 \text{ M H}_2\text{C}_2\text{O}_4$  with  $i = 8 \text{ mA cm}^{-2}$ , Nb electrode polarized for 2300 s with a final potential of 100 V after successive breakdowns.

ence of a NbO layer at the metal/oxide interface has already been reported in the literature [12]. To isolate the effect of the niobium surface, samples of oxide film were scraped off and analysed, giving the diffraction pattern presented in Fig. 6. The diffraction pattern shows that  $\text{Nb}_2\text{O}_5$  has an orthorhombic structure, which is the single phase present in the powder.

#### 4. Conclusions

The analysis of galvanostatic experiments performed on niobium electrodes in oxalic acid solutions showed that the breakdown of the anodic oxide films occurs as a consequence of the growth of internal stresses up to a limiting value that cannot be tolerated by the mechanical strength of the films. The XPS experiments confirmed the absence of  $\text{C}_2\text{O}_4^{2-}$  species incorporated in the film. A crystalline duplex film composed of NbO and  $\text{Nb}_2\text{O}_5$  was observed at the niobium surface after prolonged anodization times.

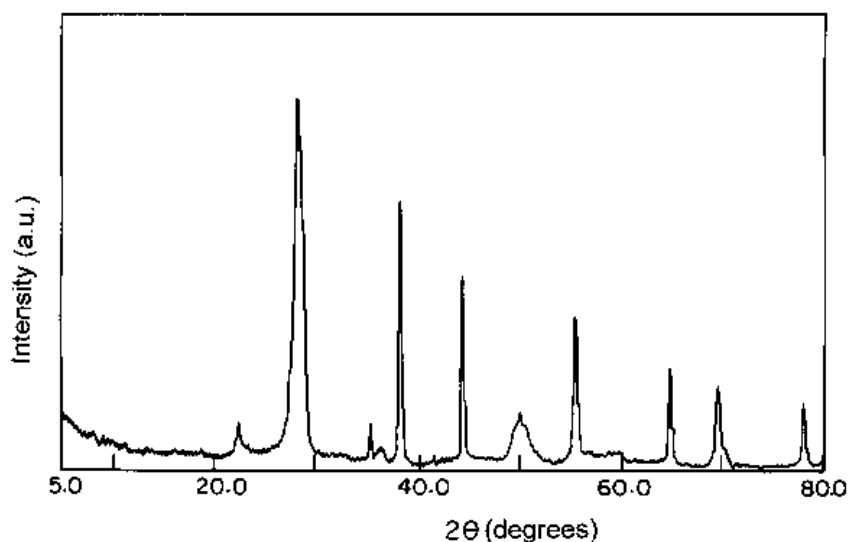


Fig. 5. The X-ray diffraction of niobium oxide film obtained during galvanostatic growth in aqueous  $0.1 \text{ M H}_2\text{C}_2\text{O}_4$  solution by applying  $18 \text{ mA cm}^{-2}$ , with an anodization time of 2000 s and a final potential of 200 V.

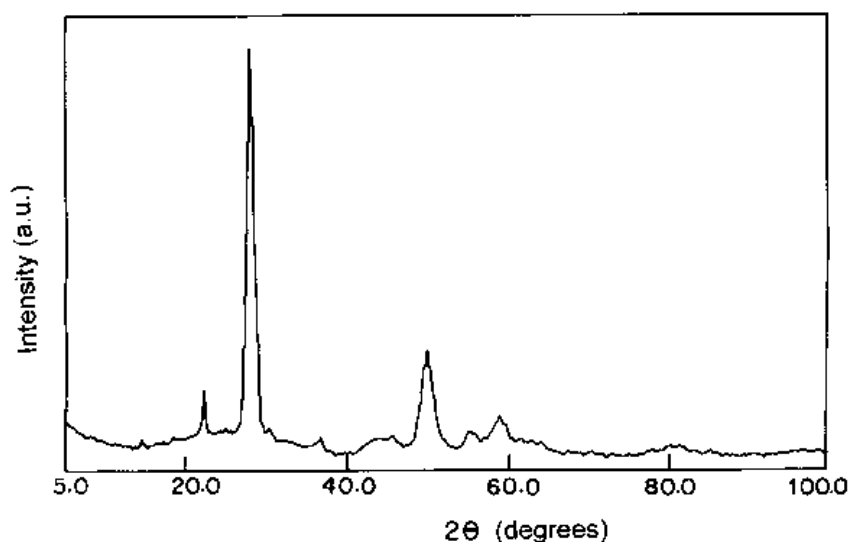


Fig. 6. The X-ray diffraction of niobium oxide film scraped from the niobium surface and obtained under conditions similar to those described for Fig. 5.

### Acknowledgements

The authors acknowledge CNPq, FAPESP and CAPES for financial support for this research.

### References

- [1] M. A. B. Gomes, S. Onofre, S. Juanto and L. O. S. Bulhões, *J. Appl. Electrochem.* **21** (1991) 1023.
- [2] F. Di Quarto, S. Piazza and C. Sunseri, *J. Electrochem. Soc.* **131** (1984) 2901.
- [3] F. Forlani and N. Minnaja, *Phys. Status Solidi* **4** (1964) 311.
- [4] S. Ikonopsov, *Electrochim. Acta* **22** (1977) 1077.
- [5] J. M. Albella, I. Monteiro and J. M. Duart, *J. Electrochem. Soc.* **131** (1984) 1101.
- [6] S. Ikonopsov, A. Girginov and M. Machkova, *Electrochim. Acta* **24** (1977) 451.
- [7] N. Sato, *ibid.* **16** (1971) 1983.
- [8] L. Young, *Trans. Faraday Soc.* **50** (1954) 153.
- [9] G. Jouve, A. Politi, P. Lacombe and G. Vuye, *J. Less Common Met.* **59** (1978) 175.
- [10] G. E. Muilenberg (ed.), 'Handbook of X-ray Photoelectron Spectroscopy', Perkin-Elmer Corp., Minnesota, USA (1978).
- [11] L. G. Berry (ed.), 'X-ray Diffraction Files', ASTM, PA, USA (1975).
- [12] J. Halbritter and M. Grunder, *J. Appl. Phys.* **51** (1980) 397.